Available online at www.sciencedirect.com
SCIENCE DIRECT®
International Journal of Multiphase Flow 30 (2004) 877–900
International Journal of Multiphase Flow
www.elsevier.com/locate/ijmulflow

Closure relations for the shear stresses in two-fluid models for laminar stratified flow ☆

A. Ullmann, A. Goldstein, M. Zamir, N. Brauner *

Faculty of Engineering, Tel-Aviv University, Tel-Aviv 69978, Israel

Received 7 July 2003; received in revised form 18 March 2004

Abstract

New closure relations for the wall and interfacial shear stresses are suggested for the two-fluid model for stratified laminar pipe flows. The new closure relations are formulated in terms of the single-phase-based expressions, which are augmented by the two-phase interaction factors.

The two-fluid model is tested against the exact solution of fully developed laminar pipe flow with a flat and smooth interface. The predictions of the two-fluid model for the pressure gradient and holdup favorably compare with those obtained by the exact solution for a wide range of dimensionless parameters in co-current and counter-current laminar flows. The two-fluid model is also capable of handling the change in the direction of the wall shear-stress when gravity driven backflow in either of the phases is encountered. Additionally, it also correctly predicts the multiple holdups and the operational conditions for their possible occurrence.

Keywords: Stratified flow; Two-fluid; Closure relations; Shear stresses; Multiple holdups

1. Introduction

Stratified flow is a basic flow pattern in horizontal and inclined gas–liquid and liquid–liquid systems in a gravity field. In case of a finite density difference between the two phases, they tend to

☆ This paper is dedicated to Prof. George Yadigaroglu on the occasion of his 65th birthday. We would like to take this opportunity to express our deep appreciation and gratitude for his invaluable contributions to research activities in the field of multiphase flow. His warm and friendly personality is greatly admired by all who know him. We wish him good luck and health in the years to come and a successful continuation of enthusiastic and fruitful research work.

* Corresponding author.
E-mail address: brauner@eng.tau.ac.il (N. Brauner).

0301-9322/$ - see front matter
doi:10.1016/j.ijmultiphaseflow.2004.03.008

segregate, and for some range of sufficiently low flow rates, a structure of continuous layers of the light phase on top of a heavy phase layer is maintained in steady and transient flows.

The key engineering parameters in the design of two-phase pipe flow are the pressure drop and average in situ holdup and velocities. Their prediction is commonly attempted via two-fluid (1-D) models, which are based on averaged momentum equations and mass conservation equations for each of the two layers. These four equations can be solved for the unknown pressure gradient, holdup and velocities of the two phases, provided closure relations are available for the wall and interfacial shear stresses. The 1-D two-fluid models are also used to study the stability of the stratified flow, for the calculation of undeveloped stratified flow and for the simulation of slow transients. Therefore, reliable and practical closure relations for the shear stresses in terms of the local and instantaneous holdup and average velocities are needed, even in cases where exact (however complicated) solutions for steady, fully developed pipe flow can be obtained.

Despite of the extensive theoretical and experimental research attempted at formulating appropriate closure laws, no models, which rigorously account for the effects of the interaction between the phases, have yet been established. The approach that is commonly followed is to use closure relations that are based on the knowledge gained in single-phase flows, and then introduce empirical corrections to match with two-phase flow data.

The vast majority of those studies relates to horizontal low-pressure gas–liquid systems, where the gas velocity is typically much higher than the liquid layer velocity and the flow phenomena is dominated by the friction in the gas phase. In liquid–liquid systems, the densities of the liquids are similar, however, a wide range viscosities is encountered. Therefore, even for horizontal flows, it is not a-priori evident which of the phases dominates the friction at the interface.

Relatively few studies relate to the closure of two-fluid models for inclined gas–liquid and liquid–liquid flows. In inclined systems, gravitational effects become important, in particular, in counter-current flows. Accurate prediction of the holdup and pressure drop requires reliable closure relations for the wall and interfacial shear stresses, which correctly represent the fine balance between frictional and gravitational forces. Multiple solutions can be obtained for specified operational conditions in co-current and counter-current inclined flows, which are relevant in practical applications (e.g. Landman, 1991; Ullmann et al., 2001; Ullmann et al., 2003a,b). It was shown in Ullmann et al. (2003a) that in inclined counter-current flows two stable stratified flow configurations of different holdups can be experimentally obtained for specified operational conditions. The feasibility of obtaining multi-holdups in co-current upflow was verified in Ullmann et al. (2003b). However, the multiple solution regions were investigated based on the two-plate model or the classical two-fluid model. The deficiencies of the conventional closure relations used in predicting the flow characteristics via two-fluid models in inclined flows is demonstrated and discussed in those references. Therefore, the boundaries of the multiple solution regions should be rechecked once robust models for inclined pipe flows become available.

In principle, the effect of the interaction between the two phases can be studied in view of exact solutions for stratified flow. These can be obtained for laminar flows, which may be of limited relevance to practical applications of gas–liquid flows in relatively large diameter conduits. However, laminar stratified flows are frequently encountered in liquid–liquid systems, and are also relevant to gas–liquid flows in the range of sufficiently low flow rates and/or small diameter tubes.

For the case of pipe geometry, exact analytical solutions for the velocity profiles $u_1(x,y)$, $u_2(x,y)$ in fully developed laminar flows can be obtained when the fluids interface can be described by a constant curvature curve. In this case, the bipolar coordinate system can be applied to obtain a complete analytical solution for the velocity profiles, distribution of shear stresses along the pipe wall and fluids interface, axial pressure drop and in situ holdup, in terms of prescribed flow rates and fluids viscosities (e.g. Bentwich, 1964; Brauner et al., 1995, 1996a for horizontal flows). The assumption of a constant curvature is practically satisfied for large Eotvos number systems, $Eo_D = \Delta\rho g D^2/8\sigma$, corresponding to large diameter (D), high density difference ($\Delta\rho$) and low surface tension (σ) systems (Brauner et al., 1996b; Brauner et al., 1998; Gorelik and Brauner, 1999). In this case, the interface is plane, with a zero pressure difference across the interface, and the flow geometry can be described by the thickness of the (lower) fluid layer, h. Analytical solutions for flow with a plane interface are given in several publications (e.g Semenov and Tochigin, 1962; Bentwich, 1964; Ranger and Davis, 1979; Brauner et al., 1996a; Biberg and Halvorsen, 2000).

Although exact expressions for the shear stresses can be obtained for steady, fully developed stratified laminar flow in inclined pipes, the computation of local stresses involve triple integrals, and additional integration is required for obtaining the averaged values (see Section 2). Therefore, from the practical point of view, they are too complicated to be implemented in two-fluid models. Moreover, the complexity of the exact solution makes it hard to identify the necessary modifications of the single-phase-based closure laws, so that the interaction between the two phases is properly accounted for. On the other hand, the exact solution obtained for the model of the simple geometry of stratified flow between two infinite plates (TP model) has been shown to be a useful tool for analyzing the characteristics of co-current and counter-current laminar pipe flows (Ullmann et al., 2003a). Therefore, the expressions obtained for the shear stresses via the TP model are re-examined to find out the structure of closure relations that are implied by this rather simple model. New closure relations evolve for the wall and interfacial shear stresses, which are then implemented into the two-fluid model (Section 3). The results of pressure gradient and holdup obtained by this modified two-fluid (MTF) model are compared with those obtained by the exact solution for laminar co-current and counter-current inclined flows. The MTF model predictions are also compared with experimental holdup data for counter-current flows (Section 4). These comparisons prove that the new closure relations are essentially representing correctly the interaction between the phases over a wide range of the stratified laminar flow parameters space.

2. Exact solution for laminar stratified flow

In two-phase stratified flows, given the location of the fluids interface, the velocity profiles of the two fluids u_1, u_2 in a steady and fully developed axial laminar flow (with a smooth interface), are obtained via analytical or numerical solutions of the following Stokes equations (in the z direction, see Fig. 1):

$$\mu_1(\nabla^2 u_1) = \frac{\mathrm{d}p}{\mathrm{d}z} - \rho_1 g \sin\beta, \quad \mu_2(\nabla^2 u_2) = \frac{\mathrm{d}p}{\mathrm{d}z} - \rho_2 g \sin\beta \tag{1}$$

The required boundary conditions follow from the no-slip condition at the pipe wall and continuity of the velocities and tangential shear stresses across the fluids' interface. For a given axial

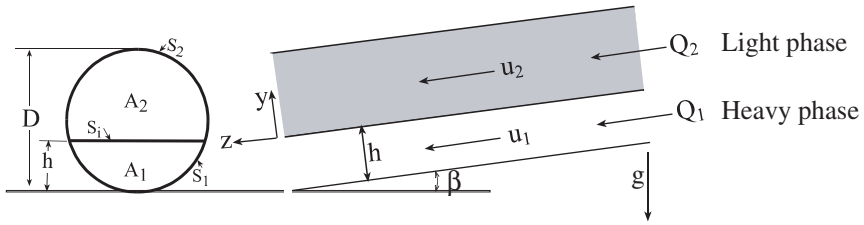

Fig. 1. Schematic description of the stratified flow configuration and coordinates.

pressure drop, the solution for u_1 and u_2 can be integrated over the fluids flow cross-sections to yield the corresponding volumetric flow rates Q_1 and Q_2. From the practical point of view, we are interested in a solution of the 'inverse problem' where the unknown pressure gradient and flow geometry (interface location) are obtained for given flow rates. However, the inverse problem is much more complicated, since the shape of fluids interface is in fact, unknown. The interface shape is obtained from the solution of the momentum equation in the y direction (Gorelik and Brauner, 1999) whereby, for large Eo_D systems the interface is flat (rather than curved). In the following, a solution of the 'inverse problem' for the case of fully developed laminar flow in inclined pipes of large Eo_D with a flat and smooth interface is presented. In particular, the focus is on obtaining a complete solution in terms of the dimensionless parameters for the case of inclined pipes. Compared to horizontal pipes, in inclined pipes the solution of the 'inverse problem' is more complicated since the driving force is different in the two phases.

2.1. Laminar pipe flow (LPF)

The appropriate coordinate system for solving the stratified flow problem in pipe geometry is the well-known bipolar coordinate system (e.g. Bentwich, 1964; Ranger and Davis, 1979). The view angle of the two triple points (interface intersection with the pipe wall) from an arbitrary point in the flow domain is $\pi - \phi$. Coordinate ξ relates to the ratio of the two radius vectors r_1, r_2 connecting the field point to the two triple points, $\xi = \ln(r_1/r_2)$. The pipe perimeter and the interface between the fluids are iso-lines of coordinates ϕ, so that the upper section of the tube wall bounding the lighter phase is represented by ϕ_2, while the bottom of the tube, bounding the denser phase, is represented by $-\phi_1 = \phi_2 - \pi$. The interface coincides with the curve of $\phi = 0$. Thus, the two-phase domains map into two infinite strips in the (ϕ, ξ) domain defined by

$$\begin{aligned} &\text{Upper phase:} \quad -\infty < \xi < \infty; \quad 0 < \phi < \phi_2 \\ &\text{Lower phase:} \quad -\infty < \xi < \infty; \quad \phi_2 - \pi < \phi < 0 \end{aligned} \tag{2}$$

Analytical solutions of the Stokes equations for inclined flows were recently explored by Goldstein (2002). Analytical expressions in terms of Fourier integrals in the bipolar coordinate system were obtained for the velocity profiles: $(\tilde{u}_{1,2} = u_{1,2}/U_{2s})$.

$$\tilde{u}_2 = \frac{u_2}{U_{2s}} = -8\widetilde{P}_2 \sin\phi_1 \left[\cos\phi_2 I_2^1 + \tilde{\mu} \sin\phi_2 I_2^2 - \frac{1}{2} \frac{\sin(\phi_2 - \phi)}{\cosh\xi + \cos\phi} \right] + 8 \sin^2\phi_2 \widetilde{P}_1 I_2^3 \tag{3.1}$$

$$\tilde{u}_1 = \frac{u_1}{U_{2s}} = -\frac{8\widetilde{P}_1}{\tilde{\mu}} \sin\phi_1 \left[\cos\phi_1 I_1^1 + \sin\phi_1 I_1^2 - \frac{1}{2} \frac{\sin(\phi_1+\phi)}{\cosh\xi + \cos\phi} \right] + 8\sin^2\phi_1 \widetilde{P}_2 I_1^3 \tag{3.2}$$

where U_{1s}, U_{2s} are the superficial phases velocities, $I_{1,2}^j$ ($j = 1, 2, 3$) denote the Fourier integrals (given in Appendix A) and:

$$\tilde{\mu} = \mu_1/\mu_2; \quad \widetilde{P}_1 = \frac{\mathrm{d}p/\mathrm{d}z - \rho_1 g \sin\beta}{(-\mathrm{d}p_f/\mathrm{d}z)_{2s}}; \quad \widetilde{P}_2 = \frac{\mathrm{d}p/\mathrm{d}z - \rho_2 g \sin\beta}{(-\mathrm{d}p_f/\mathrm{d}z)_{2s}} \tag{4}$$

While ϕ_2 (or $\phi_1 = \pi - \phi_2$) determine the geometry, $\widetilde{P}_1$ and $\widetilde{P}_2$ represent the dimensionless driving force in the heavy and light phases, respectively. The pressure gradient used for normalizing the driving forces is the frictional pressure drop obtained in single-phase flow of the lighter phase, $(-\mathrm{d}p_f/\mathrm{d}z)_{2s} = 32\mu_2 U_{2s}/D^2$. The velocity profiles, given in Eqs. (3), are in fact the same as the (dimensional) profile obtained by Biberg and Halvorsen (2000) for inclined flows. In order to obtain the holdup and the pressure gradient for a given two-fluid system and flow rates, a solution for the 'inverse problem' must to be obtained.

The total pressure drop is composed of the gravitational (hydrostatic) pressure drop, which is determined by the holdup, and the frictional pressure drop. The $\widetilde{P}_1$ and $\widetilde{P}_2$ are both unknown, as they relate to the (unknown) total pressure drop. The difference between the two, however, is equal to the inclination parameter, Y:

$$\widetilde{P}_2 - \widetilde{P}_1 = \frac{(\rho_1 - \rho_2) g \sin\beta}{(-\mathrm{d}p_f/\mathrm{d}z)_{2s}} = Y \tag{5}$$

The form used in Eqs. (3) clearly shows that the unknown $\widetilde{P}_1$ and $\widetilde{P}_2$ can be obtained from these two equations after integration of the velocity profiles over the corresponding flow cross-sectional area to provide the (known) flow rates of the two fluids. Accordingly:

$$\frac{1}{\pi} \int_0^{\phi_2} \int_{-\infty}^{\infty} \tilde{u}_2 J(\xi,\phi)\, \mathrm{d}\xi\, \mathrm{d}\phi = 1 \tag{6.1}$$

$$\frac{1}{\pi} \int_{-\phi_1}^{0} \int_{-\infty}^{\infty} \tilde{u}_1 J(\xi,\phi)\, \mathrm{d}\xi\, \mathrm{d}\phi = q = \frac{U_{1s}}{U_{2s}} \tag{6.2}$$

where $J(\xi,\phi)$ is the transforming Jacobian from bipolar to Cartesian coordinates:

$$J(\xi,\phi) = \frac{-\sin^2\phi_1}{(\cosh\xi + \cos\phi)^2} \tag{6.3}$$

Eqs. (6) can be solved for the unknown $\widetilde{P}_1$, $\widetilde{P}_2$. The solutions so obtained are given by

$$\widetilde{P}_2 = \frac{\pi}{8\sin\phi_1} \frac{I_1^{A5} + \tilde{\mu} q I_2^{A3}}{[I_1^{A5} I_2^{A5} - \tilde{\mu} I_1^{A3} I_2^{A3}]} \tag{7.1}$$

$$\widetilde{P}_1 = \frac{-\pi}{8\sin\phi_1} \left\{ \frac{[I_1^{A5} + \tilde{\mu} q I_2^{A3}] \tilde{\mu} I_1^{A3}}{I_1^{A5}[I_1^{A5} I_2^{A5} - \tilde{\mu} I_1^{A3} I_2^{A3}]} + \frac{\tilde{\mu} q}{I_1^{A5}} \right\} \tag{7.2}$$

and by Eq. (5):

$$X^2 = \tilde{\mu} q = \frac{\left(\frac{8}{\pi}\sin\phi_1 I^{A7} Y + I^{A6}\right) I_1^{A5}}{\left(I^{A7} - I_2^{A3} I^{A6}\right)} \tag{8}$$

where the various $I_{1,2}^{Aj}$ terms represents triple integrals (over the ω, ϕ and ξ domains), which are defined in Appendix A. Note that $X^2 = (-\mathrm{d}p_\mathrm{f}/\mathrm{d}z)_{1\mathrm{s}}/(-\mathrm{d}p_\mathrm{f}/\mathrm{d}z)_{2\mathrm{s}} = \tilde{\mu} q$ is the Martinelli parameter in the case of laminar flow.

Eq. (8) represents an implicit relation between the unknown holdup, $\varepsilon = 4A_1/\pi D^2$ (determined by $\phi_1, \phi_2 = \pi - \phi_1$) and the three prescribed dimensionless parameters $\tilde{\mu}$, q and Y (or X^2, $\tilde{\mu}$ and Y). These are obviously the same three dimensionless parameters that evolve from the two-fluid model (Ullmann et al., 2003a). Note that the inclination angle, β is always taken as positive. In co-current flow, $U_{1\mathrm{s}}$, $U_{2\mathrm{s}}$ are both positive in case of downward flow and negative for the case of upward flow. Whereas in counter-current flow $U_{2\mathrm{s}}$ is negative (the light phase flows upward). Accordingly, co-current flows correspond to $X^2 > 0$ with $Y > 0 (< 0)$ for down-flow (up-flow). Counter-current flows correspond to $X^2 < 0$ and $Y < 0$. The solutions of Eq. (8) comply with the natural symmetry which exists between upward (A) and downward (B) two-phase flow systems: if $(q)_A = (1/q)_B$, $(\tilde{\mu})_A = (1/\tilde{\mu})_B$ and $(Y)_A = (Y/X^2)_B$, then $\varepsilon_A = (1-\varepsilon)_B$ (see also Brauner et al., 1996a; Ullmann et al., 2003b).

The total pressure drop is composed of the gravitational (hydrostatic) pressure drop, which is determined by the holdup:

$$\left(\frac{\mathrm{d}p_\mathrm{g}}{\mathrm{d}z}\right) = [\rho_1\varepsilon + \rho_2(1-\varepsilon)]g\sin\beta = [\rho_2 + (\rho_1 - \rho_2)\varepsilon]g\sin\beta \tag{9}$$

and the frictional pressure gradient, $(-\mathrm{d}p_\mathrm{f}/\mathrm{d}z)$. In terms of the solution dimensionless parameters, the dimensionless frictional pressure gradient, Π_f and the additional hydrostatic pressure gradient (compared to single phase flow of the light phase) are given by:

$$\Pi_\mathrm{f} = -\frac{\mathrm{d}p/\mathrm{d}z - (\mathrm{d}p_\mathrm{g}/\mathrm{d}z)}{(-\mathrm{d}p_\mathrm{f}/\mathrm{d}z)_{2\mathrm{s}}} = -\widetilde{P}_2 + Y\varepsilon \tag{10.1}$$

$$\Pi_\mathrm{g} = \frac{(\mathrm{d}p/\mathrm{d}z) - (\mathrm{d}p_\mathrm{g}/\mathrm{d}z)_{2\mathrm{s}}}{(-\mathrm{d}p_\mathrm{f}/\mathrm{d}z)_{2\mathrm{s}}} = Y\varepsilon \tag{10.2}$$

The local shear stresses are obtained by differentiation of the velocity profiles. The expressions obtained for the dimensionless wall shear stresses τ_1 at $\phi = -\phi_1$ and τ_2 at $\phi = \phi_2$ read:

$$\tilde{\tau}_1^{\xi} = \frac{\tau_1(\xi)}{\tau_{2\mathrm{s}}} = \widetilde{P}_1\left\{1 - 2(\cosh\xi + \cosh\phi_1)\int_0^\infty \left[\cos\phi_1 - \frac{\psi_1(\omega)}{\psi(\omega)}\right] W_{1\tau}\,\mathrm{d}\omega\right\} + 2\widetilde{P}_2\tilde{\mu}(\cosh\xi + \cos\phi_1)\int_0^\infty \frac{\psi_2(\omega)}{\psi(\omega)} W_{1\tau}\,\mathrm{d}\omega \tag{11.1}$$

$$\tilde{\tau}_2^{\xi} = \frac{\tau_2(\xi)}{\tau_{2\mathrm{s}}} = \widetilde{P}_2\left\{1 - (\cosh\xi + \cos\phi_2)\int_0^\infty \left[\cos\phi_2 - \tilde{\mu}\frac{\psi_2(\omega)}{\psi(\omega)}\right] W_{2\tau}\,\mathrm{d}\omega\right\} + 2\widetilde{P}_1(\cosh\xi + \cos\phi_2)\int_0^\infty \frac{\psi_1(\omega)}{\psi(\omega)} W_{2\tau}\,\mathrm{d}\omega \tag{11.2}$$

where:

$$W_{1\tau} = \frac{\omega\cos(\omega\xi)}{\sinh(\omega\pi)\cosh(\omega\phi_1)}; \quad W_{2\tau} = \frac{\omega\cos(\omega\xi)}{\sinh(\omega\pi)\cosh(\omega\phi_2)}$$
$$\tau_{2s} = \frac{R}{2}\left(-\frac{\mathrm{d}p_f}{\mathrm{d}z}\right)_{2s} \tag{11.3}$$

and the functions ψ_1, ψ_2 and ψ are given in Appendix A. The average wall shear stresses are obtained by integration of the local value over the wetted perimeters:

$$\tilde{\tau}_1 = \sin\phi_1 \int_{-\infty}^{\infty} \frac{\tilde{\tau}_1^{\xi}}{\cosh\xi + \cos\phi_1}\,\mathrm{d}\xi; \quad \tilde{\tau}_2 = \sin\phi_2 \int_{-\infty}^{\infty} \frac{\tilde{\tau}_2^{\xi}}{\cosh\xi + \cos\phi_2}\,\mathrm{d}\xi \tag{12}$$

The local shear stress at the fluid interface, $\phi = 0$, is given by

$$\tilde{\tau}_i^{\xi} = \frac{\tau_i(\xi)}{\tau_{2s}} = -4\sin\phi_1\cosh^2\left(\frac{\xi}{2}\right)\int_0^{\infty}\left\{\frac{\widetilde{P}_1\psi_1(\omega) - \tilde{\mu}\widetilde{P}_2\psi_2(\omega)}{\psi(\omega)}\right\}\frac{\omega\cos(\omega\xi)}{\sinh(\omega\pi)}\,\mathrm{d}\omega \tag{13}$$

and the average interfacial shear stress:

$$\tilde{\tau}_i = \frac{\tau_i}{\tau_{2s}} = \sin\phi_1\int_{-\infty}^{\infty}\frac{\tau_i^{\xi}}{\cosh\xi + 1}\,\mathrm{d}\xi \tag{14}$$

The effects of the viscosity ratio and holdup on the wall and interfacial shear stress profiles in horizontal flows were explored in Brauner et al. (1996a) and Moalem-Maron et al. (1995) and more recently by Biberg and Halvorsen (2000) and Goldstein (2002) for the case of inclined flows. It was shown that the wall shear stresses may not be continuous at the fluids interface (at the triple points). Their values may explode as the triple points are approached, and so may also the interfacial shear. Regular variation at the vicinity of the triple points is only obtained in cases where the sharp angle between the interface and the tube wall is in the more viscous fluid (Moalem-Maron et al., 1995). However, in all cases, the averaged values of τ_1, τ_2 and τ_i are finite.

2.2. Comparison of two-fluid (TF) predictions with LPF exact solution

The LPF exact solution can be used to test the validity of two-fluid models predictions when applied to cases of fully developed laminar stratified flow with a flat and smooth interface. The poor predictions obtained when the conventional single-phase-based closure relations (TF model) are applied to predict experimental data of counter-current liquid–liquid flow has been shown in Ullmann et al. (2003a). The details of the closure relations used in the co-current and counter-current regions are given in that reference. In Fig. 2, the TF model results are demonstrated for a test case of liquid–liquid laminar flow corresponding to a shallow inclination of $\beta = 5.5°$ and constant $Q_1(Y/X^2 = 18)$.

In the parameter space where counter-current flows are feasible, there are two possible configurations for specified operational conditions that merge into a single one at the ultimate flooding point. The data shown in Fig. 2 correspond to the two stable stratified flow

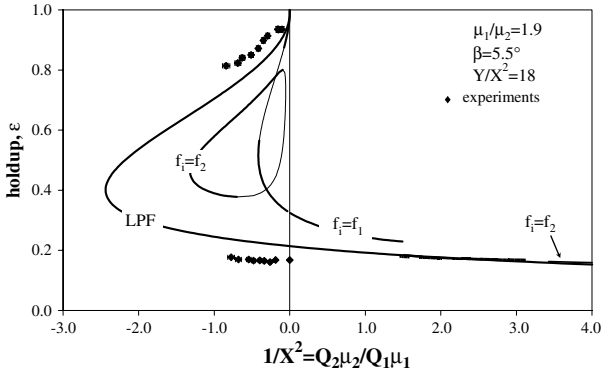

Fig. 2. Comparison of the LPF solution for the holdup with the results of the TF model for the case of $\beta = 5.5°$ and $\tilde{\mu} = 1.9$ (bold lines—$f_i = f_2$ for $|U_2| > |U_1$ and $f_i = f_1$ for $|U_1| > |U_2|$; dashed line—'free interface' assumed in the hydraulic diameter calculation of both phases). Data correspond to counter current flow $\rho_1 = 953.6$, $\rho_2 = 910.4$ kg/m^3, $\mu_1 = 3.25 \times 10^{-3}$ kg/m/s, $Q_1 = 42.5 \pm 2$ ml/min, $Re_{1s} = 19$, $Re_{2s} = 5.5$–45 and $Eo_D \approx 2.5$ (Ullmann et al., 2003a).

configurations that were obtained in the experiments. It is worth emphasizing that all the data are for laminar flow in both of the phases, with a flat and smooth interface. Therefore, possible effects of turbulence, interface curvature, interfacial waves and drop entrainment are ruled out.

The TF model predictions for the counter-current holdup curve are shown for two possible cases where the interfacial shear is considered to be controlled either by the flow of the light phase (the interfacial friction factor is assumed to be equal to the wall friction factor of the lighter phase, $f_i = f_2$) or by the flow of the heavy phase, ($f_i = f_1$). In principle, each of these models for the interfacial shear can provide up to two solutions for the holdup in counter-current flow. It is worth noting that in the range of $1/X^2 \to 0$, no solution is obtained with $f_i = f_2$, whereas for relatively high $1/X^2$ no solution is obtained with $f_i = f_1$. However, there is a range of flow rates where four solutions coexist. The segments of the holdup curves, where the velocity of the phase that controls the interfacial shear is higher than the other phase (and presumably controls the interfacial shear), are marked as bold lines. Adopting a criterion based on the ratio of the absolute phase velocities for switching between the solutions, reduces the number of solutions on one hand, but on the other hand, eliminates valid solutions and introduces discontinuities. Note that discontinuity in the TF model solutions is encountered also in the co-current region, in the transition between heavy phase dominance (low $1/X^2$) to light phase dominance (high $1/X^2$) of f_i. This discontinuity corresponds to a range of flow rates where the velocities of the two phases are similar. In this range, a solution can be obtained only if the interface is considered as 'free' (not included in the wetted perimeter) in the calculation of the hydraulic diameters of both phases (see also Brauner and Moalem Maron, 1989).

Results of the LPF solution for this test case are also shown in Fig. 2. The counter-current region implied by the exact solution is significantly larger than that obtained by the two (different) curves of the TF model (when applied with either $f_i = f_1$ or $f_i = f_2$). The discrepancies between the holdup data and the exact solution are much lower compared to those indicated by the TF model predictions. Yet, the source of these discrepancies remains unclear. These cannot be attributed to wave effects or other possible irregularities at the interface, since as already men-

tioned, the interface in the experiments was definitely observed as being smooth and flat. Also, no measurable holdup gradient could be detected in the test section where holdup measurements were taken (see Ullmann et al., 2003a). Still, the possibility that for shallow inclinations a much longer pipe is required to establish the fully developed conditions cannot be ruled out. It is also worth noting that surface tension gradients along the interface (due to possible presence of minute amounts of contaminants) can give rise to an additional interfacial shear. In such a case, the length of the developing region is dominated by the rather slow diffusion process.

Obviously, the erroneous results of the TF model for the holdup yield also erroneous values for the gravitational pressure gradient, which is the major contribution to the total pressure drop in inclined systems. In this test case, the frictional pressure gradient is less than 0.5% of the total pressure gradient in the counter-current, and about 1.5% in the co-current region. A comparison of the LPF results for the frictional pressure gradient with those obtained by the TF model is shown in Fig. 3. The problematic choice of the interfacial friction factor in the TF model, as discussed with reference to the holdup predictions, have obvious implications also on the prediction of the pressure drop.

The above test case demonstrates the problems that may be encountered in applying the TF model for the prediction of the stratified flow characteristics, even for the relatively simple case of fully developed laminar flows with a smooth and flat interface. The complications and poor predictions evolve from the inherent inaccuracy of the closure laws used for the shear stresses and, in particular, the interfacial shear stress. In gas–liquid (horizontal and upward inclined) systems, the gas phase is typically turbulent and its velocity is much larger than that of the liquid layer. The interfacial friction factor is then evaluated based on the wall friction factor of the gas phase. A crucial issue in applying the two-fluid model to gas–liquid systems is frequently the modeling of a correction factor, which accounts for the augmentation of the interfacial shear due to the wavy liquid interface. However, in the general case of inclined flows, counter-current flows and liquid–liquid systems, where velocities of the two-phases are of comparable values, the main issue concerns the decision as to which of the fluids actually dominates the interfacial interaction, hence

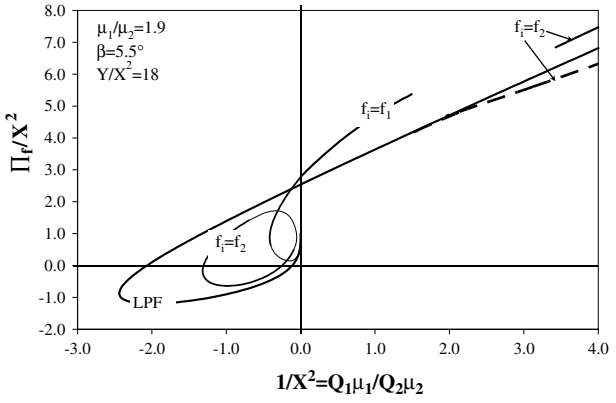

Fig. 3. Comparison of the LPF solution for the dimensionless frictional pressure gradient with the results of the TF model for $\beta = 5.5°$ and $\tilde{\mu} = 1.9$ (bold lines—$f_i = f_2$ for $|U_2| > |U_1|$ and $f_i = f_1$ for $|U_1| > |U_2|$; dashed line—'free interface' assumed in the hydraulic diameter calculation of both phases).

f_i. The commonly used wall shear expressions are also problematic for inclined flow, since they are incapable of representing reversed wall shear in cases of backflow of one of the phases in the near wall region (e.g. downward flow of the liquid phase near the wall in co-current upward gas–liquid flows).

In fact, the structures of the closure relations, which are borrowed from single phase theory/correlations, are incapable of representing correctly the interaction between the two phases. This calls for re-examination of the closure laws for the shear stresses and their improvement based on structures implied by exact solutions of laminar stratified flows.

The question is whether the LPF exact solutions for the wall and interfacial shear stresses provide a clue as to what modifications are required in the structure of the closure relations for the shear stresses used in the two-fluid model. Recalling that an appropriate closure relation for the two-fluid model is one that relates the average shear stress to the in situ holdup and velocities, however, not to the pressure drop, the $\widetilde{P}_1$ and $\widetilde{P}_2$ terms should be first eliminated from Eqs. (11) and (13) (using Eqs. (7)). Then, integration over the corresponding wetted perimeters must be carried out to obtain the averaged values for the shear stresses. Inspection of the expressions that eventually evolve (not shown) reveals that they are far too complex to be of any direct usefulness for obtaining closure relations for the two-fluid model. Therefore, it is of interest to explore the exact solution for the shear stresses obtained in a simpler geometry of the flow between two-plates. This is in order to understand how the interaction between the phases is represented by the expressions obtained for the shear stresses in this model.

2.3. Closure relations based on the two-plate (TP) model

The laminar two-phase flow between two parallel plates is a simple model, which has been proven to be a useful tool for analyzing the characteristics of stratified flow in inclined channels. For this geometry, $\partial^2 u_{1,2}/\partial x^2 = 0$ in the NS equations (1), and the solution for the velocity profiles and shear stresses is straightforward (e.g. Ullmann et al., 2003a). Here, the expressions obtained for the wall shear stresses via the TP model are cast into the following forms:

$$\tau_1 = -\frac{1}{2}\rho_1 f_1 |U_1| U_1 \cdot F_1 \tag{15.1}$$

$$F_1 = \frac{1+\frac{1}{2}\frac{U_2}{U_1}\left[\tilde{\mu}\frac{U_1}{U_2}\frac{(1-\tilde{h})}{\tilde{h}}-1\right]}{1+\tilde{\mu}\left(\frac{1-\tilde{h}}{\tilde{h}}\right)} = \frac{1+\frac{1}{2}\frac{U_2}{U_1}\left[\tilde{\mu}q\left(\frac{1-\tilde{h}}{\tilde{h}}\right)^2-1\right]}{1+\frac{U_2}{U_1}\tilde{\mu}q\left(\frac{1-\tilde{h}}{\tilde{h}}\right)^2} \tag{15.2}$$

and

$$\tau_2 = -\frac{1}{2}\rho_2 f_2 |U_2| U_2 \cdot F_2 \tag{16.1}$$

$$F_2 = \frac{1+\frac{1}{2}\frac{U_1}{U_2}\left[\frac{1}{\tilde{\mu}}\frac{U_2}{U_1}\frac{\tilde{h}}{(1-\tilde{h})}-1\right]}{1+\frac{1}{\tilde{\mu}}\frac{\tilde{h}}{(1-\tilde{h})}} = \frac{1+\frac{1}{2}\frac{U_1}{U_2}\left[\frac{1}{\tilde{\mu}q}\left(\frac{\tilde{h}}{1-\tilde{h}}\right)^2-1\right]}{1+\frac{U_1}{U_2}\frac{1}{\tilde{\mu}q}\left(\frac{\tilde{h}}{1-\tilde{h}}\right)^2} \tag{16.2}$$

where $\tilde{h} = h/H$ is the dimensionless heavier layer thickness (H denoted the distance between the plates). The average velocities U_1, U_2 are positive (negative) for downward (upward) flows. The friction factors f_1 and f_2 are based on the Reynolds number of the corresponding layer:

$$f_1 = \frac{24}{Re_1}; \quad Re_1 = \frac{\rho_1 |U_1| D_1}{\mu_1}; \quad D_1 = 2h \tag{17.1}$$

$$f_2 = \frac{24}{Re_2}; \quad Re_2 = \frac{\rho_1 |U_2| D_2}{\mu_2}; \quad D_2 = 2(H-h) \tag{17.2}$$

It is worth noting that the hydraulic diameter D_1, D_2, used in Re_1 and Re_2 respectively, are defined by considering the fluids interface as a wetted (rather than free) surface with respect to the flow of both layers. The F_1 and F_2 terms in Eqs. (15) and (16) represent correction factors, which represent the effects of the interaction between the two fluids flowing in the same channel on the wall shear stress. Evidently, these F-interaction terms may attain negative values and thus correctly represent the occurrence of reversed wall shear in cases of near wall back-flow in inclined flows.

For $F_1 = 1$ (or $F_2 = 1$) the wall shear stress correspond to that obtained in single-phase flow of the lower (or upper) fluid through two-plates spaced by the layer thickness, h (or $H - h$). Indeed, as $U_1/U_2 \to 0$ (whereby $\frac{U_1}{U_2}\left[\frac{1}{\tilde{\mu}q}\left(\frac{\tilde{h}}{1-\tilde{h}}\right)^2 - 1\right] \to 0$), Eq. (16.2) yields $F_2 \to 1$. In this case the interface can be considered as a wall with respect to the upper phase and the wall friction factor can be modeled based on single phase correlations for the friction factor. This is a typical case in gas–liquid horizontal and upward inclined systems, where the gas velocity is usually much higher than the liquid velocity. In such cases of $U_2/U_1 \gg 1$, and where also $\tilde{\mu}q(1-\tilde{h})^2/\tilde{h}^2 \gg 1$, Eq. (15.2) renders $F_1 \to 1/2$. Hence, for the slower heavier (liquid) phase, the effective wall friction factor is half the single-phase friction factor (f_1), corresponding to an increase of the hydraulic diameter D_2 by a factor of 2. In the TF model, this is equivalent to considering the interface as free while modeling the hydraulic diameter, D_2. Obviously, similar arguments apply for the opposite case of $U_2/U_1 \ll 1$, where the heavier fluid is the faster whereby $F_1 \to 1$ and $F_2 \to 1/2$.

The interfacial shear stress in the TP model can be cast into either of the following two forms:

$$\tau_i = -\frac{1}{2}\rho_1 f_1 |U_1|(U_2 - U_1) \cdot F_{i1} \tag{18.1}$$

with

$$F_{i1} = \frac{1}{1 + \tilde{\mu}\left(\frac{1-\tilde{h}}{\tilde{h}}\right)} = \frac{1}{1 + \frac{U_2}{U_1}\tilde{\mu}q\left(\frac{1-\tilde{h}}{\tilde{h}}\right)^2} \tag{18.2}$$

or equivalently:

$$\tau_i = -\frac{1}{2}\rho_2 f_2 |U_2|(U_2 - U_1) \cdot F_{i2} \tag{19.1}$$

with

$$F_{i2} = \frac{1}{1 + \frac{1}{\tilde{\mu}}\left(\frac{\tilde{h}}{1-\tilde{h}}\right)} = \frac{1}{1 + \frac{U_1}{U_2}\frac{1}{\tilde{\mu}q}\left(\frac{\tilde{h}}{1-\tilde{h}}\right)^2} \tag{19.2}$$

The first point worth noting concerns the structure of the closure relation for τ_i implied by the TP model. The structure of τ_i suggests that if it is based on the wall friction factor of either of the fluids, the τ_i should be modeled based on the velocity difference times the velocity of the selected fluid (rather than the commonly used structure, where the square of the velocity difference is used). The F_i represents a correction factor due to the interaction between the flows in the two layers. The use of the first form with F_{i1} is convenient in cases of a much faster or less viscous lower layer, where $U_2/U_1 \to 0$ $\left(\text{and } \frac{U_2}{U_1}\tilde{\mu}q\left(\frac{1-\tilde{h}}{\tilde{h}}\right)^2 \to 0\right)$. In this case $F_{i1} \to 1$ and the interfacial shear stress is in fact dominated by the flow of the lower-layer. On the other hand, in the opposite case of a much faster upper layer, $U_1/U_2 \to 0\left(\text{and } \frac{U_1}{U_2}\frac{1}{\tilde{\mu}q}\left(\frac{\tilde{h}}{1-\tilde{h}}\right)^2 \to 0\right)$. Then $F_{i2} \to 1$, indicating that the interfacial shear stress is dominated by the flow of upper layer.

Obviously, by applying the integral combined momentum equation (Eq. (21) below) for the two-plates geometry with the above closure laws for the wall and the interfacial shear stresses (Eqs. (15), (16), and (18) or (19)), the exact results for the holdup and pressure drop in the TP model are reproduced. Either of the above two expressions for the interfacial shear stress can be used. However, representing the interfacial shear stress based on the flow of the slower (or more viscous) layer, (namely using f_2 to model τ_i in cases of $\frac{U_1}{U_2}\frac{1}{\tilde{\mu}q}\left(\frac{\tilde{h}}{1-\tilde{h}}\right)^2 \gg 1$, or f_1 cases $\frac{U_2}{U_1}\tilde{\mu}q\left(\frac{1-\tilde{h}}{\tilde{h}}\right)^2 \gg 1$), requires major corrections of the single-phase friction factors to correctly represent the interaction between the two layers. These correction factors must then be rigorously accounted to correctly predict the pressure drop and holdup. Hence, it is preferable to present the interfacial shear stress based on the layer associated with the F_i being closer to 1.

The structure of the closure laws that evolves from the TP model for the wall shear stresses provides some justification to the conventional single-phase-based closure relations used in two-fluid models, when these are applied to horizontal flows in the extremes of either $U_1/U_2 \to 0$ or $U_2/U_1 \to 0$. However, F_1 and F_2 (Eqs. (15.2) and (16.2)) suggest a possible structure for the correction factors on the single-phase-based friction factor models/correlations, which plausibly account for the interaction between the two fluids.

As a first test for the relevance of the TP closure relations to pipe flow, these are implemented in the two-fluid momentum equations with some called-for modifications: the $\tilde{h}$ in Eqs. (15.2), (16.2), (18.2) and (19.2) is interpreted as the heavier fluid holdup, $\varepsilon = A_1/A$ and the wall friction factors are calculated based on laminar pipe flow, $f_{1,2} = 16/Re_{1,2}$. Figs. 4a and b show the results obtained for the holdup and for the frictional pressure gradient by this model (denoted in the figures, by TF(TP)), in comparison with the LPF solution and the TP model results. Indeed, as demonstrated in Fig. 4a, the two-fluid model predictions for the holdup are dramatically improved by the inclusion of the above F-interaction factors. The entire holdup curve is now close to that obtained by the LPF exact solution. This reflects the fact that the velocity profiles at the pipe centerline (in inclined and horizontal flows) exhibit similar characteristics to those obtained with the TP model, when the two geometries are compared for the same holdup (see Ullmann et al., 2003a). However, the comparison of the frictional pressure gradient with the LPF solution (Fig. 4b) is less favorable. As expected, the pressure gradients are more sensitive to the different wetted perimeter's ratios in the TP and pipe geometries. Further adjustments of the F-interaction factors to account for the geometrical differences are suggested in the following section, where the full set of equations of the modified two-fluid model is presented.

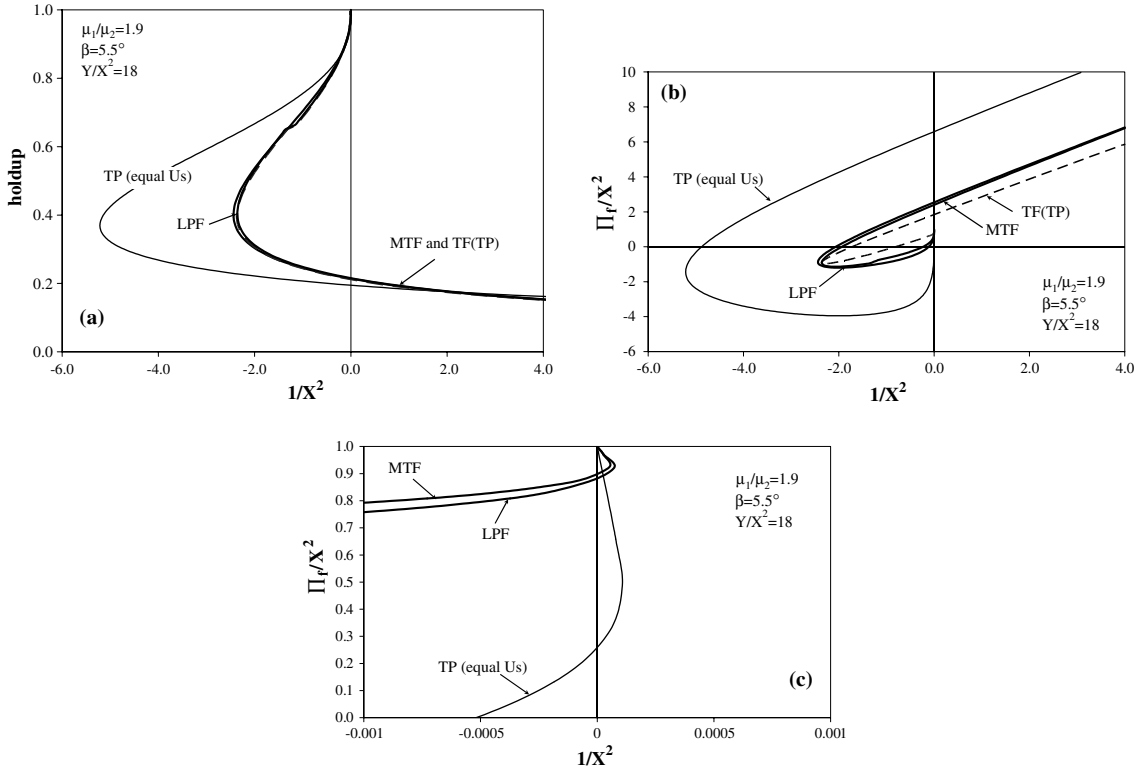

Fig. 4. Comparison of the TF(TP) and the MTF model with the LPF and TP models for ($\beta = 5.5°$ and $\tilde{\mu} = 1.9$): (a) Holdup, (b) dimensionless frictional pressure gradient, (c) magnification of the small $1/X^2$ region in Fig. 4b. (TP (equal Us)—TP model applied for the same superficial velocity as in pipe flow).

3. The modified two-fluid (MTF) model

Assuming a fully developed stratified flow, the integral forms of the momentum equations for the two fluids are (see Fig. 1):

$$-A_1 \frac{\mathrm{d}p}{\mathrm{d}z} + \tau_1 S_1 - \tau_i S_i + \rho_1 A_1 g \sin\beta = 0 \tag{20.1}$$

$$-A_2 \frac{\mathrm{d}p}{\mathrm{d}z} + \tau_2 S_2 + \tau_i S_i + \rho_2 A_2 g \sin\beta = 0 \tag{20.2}$$

where $A_{1,2}$ and $S_{1,2}$ are the cross-sectional area and the wall perimeter of each of the fluids respectively and S_i is the interfacial perimeter (see Fig. 1). Eliminating the pressure drop yields:

$$\tau_1 \frac{S_1}{A_1} - \tau_2 \frac{S_2}{A_2} - \tau_i S_i \left(\frac{1}{A_1} + \frac{1}{A_2} \right) + (\rho_1 - \rho_2) g \sin\beta = 0 \tag{21}$$

The closure relations adopted for the wall and interfacial shear stresses are basically those presented in Section 2.3 based on the TP model. However, due to the different geometries involved, some further adjustments are obviously necessary when the F-interaction factors are applied to

pipe flow. In fact, the factor 1/2 in the numerator of F_1 and F_2 (see Eqs. (15.2) and (16.2)) can represent various relations of the wetted perimeters and the interface width in the TP geometry (e.g. $S_{1,2}/(S_1+S_2)$, $S_i/(S_1+S_2)$, $S_{1,2}/(S_i+S_{1,2})$). This is not the case for pipe geometry. Recalling that in laminar flows $X^2=\tilde{\mu}q$, the following closure relations are suggested for pipe flow:

$$\tau_1=-\frac{1}{2}\rho_1 f_1|U_1|U_1F_1;\quad F_1=\frac{1+\frac{U_2}{U_1}\left[g_{11}X^2\left(\frac{1-\varepsilon}{\varepsilon}\right)^2-g_{12}\right]}{1+\frac{U_2}{U_1}X^2\left(\frac{1-\varepsilon}{\varepsilon}\right)^2} \tag{22.1}$$

$$\tau_2=-\frac{1}{2}\rho_2 f_2|U_2|U_2F_2;\quad F_2=\frac{1+\frac{U_1}{U_2}\left[g_{22}\frac{1}{X^2}\left(\frac{\varepsilon}{1-\varepsilon}\right)^2-g_{21}\right]}{1+\frac{U_1}{U_2}\frac{1}{X^2}\left(\frac{\varepsilon}{1-\varepsilon}\right)^2} \tag{22.2}$$

with

$$f_1=\frac{16}{Re_1};\quad Re_1=\frac{\rho_1|U_1|D_1}{\mu_1};\quad D_1=\frac{4A_1}{(S_1+S_i)}=\pi D\frac{\varepsilon_1}{\widetilde{S}_1+\widetilde{S}_i} \tag{23.1}$$

$$f_2=\frac{16}{Re_2};\quad Re_2=\frac{\rho_2|U_2|D_2}{\mu_2};\quad D_2=\frac{4A_2}{(S_2+S_i)}=\pi D\frac{\varepsilon_2}{\widetilde{S}_2+\widetilde{S}_i} \tag{23.2}$$

The g_{11}, g_{12}, g_{21}, g_{22} are functions of the dimensionless wetted perimeters $\widetilde{S}_1$, $\widetilde{S}_2$ and $\widetilde{S}_i$ in the pipe geometry, ($\widetilde{S}=S/D$). These functions are determined based on the closure relations expected for τ_1 and τ_2 in some limiting cases. To make the hydraulic diameter of the much slower layer converge to the value corresponding to the free interface model (see the discussion related to Eqs. (15) and (16)), the following g_{11} and g_{22} are implemented:

$$g_{11}=\frac{\widetilde{S}_1}{\widetilde{S}_1+\widetilde{S}_i};\quad g_{22}=\frac{\widetilde{S}_2}{\widetilde{S}_2+\widetilde{S}_i} \tag{24.1}$$

The functions g_{12} and g_{21} are set to render the correct value of the shear stress in the particular case of $\tilde{\mu}=1$, $q=1$ and $\varepsilon=1/2$ (corresponding to single-phase laminar pipe flow, $\tau_1=\tau_2=8\mu_{1,2}U_{1,2}/D$), and to follow the trend of τ_1 (or τ_2) as $X^2\to 0$ (or $1/X^2\to 0$):

$$g_{12}=\frac{4}{\pi+2}\frac{\widetilde{S}_2}{\widetilde{S}_2+\widetilde{S}_1};\quad g_{21}=\frac{4}{\pi+2}\frac{\widetilde{S}_1}{\widetilde{S}_2+\widetilde{S}_1} \tag{24.2}$$

For the interfacial shear, the following closure relations evolve from Eqs. (18) and (19) for pipe flow:

$$\tau_i=\begin{cases}-\frac{1}{2}\rho_1 f_1|U_1|(U_2-U_1)F_{i1}; & \frac{U_2}{U_1}X^2\left(\frac{1-\varepsilon}{\varepsilon}\right)^2\leqslant\frac{U_1}{U_2}\frac{1}{X^2}\left(\frac{\varepsilon}{1-\varepsilon}\right)^2\\ -\frac{1}{2}\rho_2 f_2|U_2|(U_2-U_1)F_{i2}; & \frac{U_2}{U_1}X^2\left(\frac{1-\varepsilon}{\varepsilon}\right)^2>\frac{U_1}{U_2}\frac{1}{X^2}\left(\frac{\varepsilon}{1-\varepsilon}\right)^2\end{cases} \tag{25}$$

The first line in Eq. (25) corresponds to the case where the interfacial shear is dominated by the flow of the heavy phase, whereas the second line corresponds to dominance by the light phase. The criterion used in Eq. (25) to switch between the two alternative expressions suggests a matching between the solutions for these two cases. The MTF closure relation for the interfacial shear thus avoids the discontinuity and other ill effects encountered in the TF predictions.

The two-fluid momentum equations (Eqs. (20)), when combined with the closure relations given in Eqs. (22)–(25), comprise the modified two-fluid (MTF) model. Note that upon substituting the above closure relations in the combined momentum equation (21), and using dimensionless variables, an implicit relation of the dimensionless heavier layer thickness $\tilde{h} = h/D$ is obtained, $f(X^2, Y, q, \tilde{h}) = 0$. This relation is the equivalence of Eq. (8) in the LPF exact solution. Once a solution has been obtained for the holdup, the corresponding pressure drop can be calculated either of Eqs. (20), or from their sum.

4. Validation of the modified two-fluid (MTF) model-discussion

The results of the MTF model for the test case of 5.5° are shown in Fig. 4 in comparison to the LPF solution. Both the holdup and the frictional pressure gradient are close to the values obtained by the LPF solution in the counter-current and co-current regions. It is of interest to observe the detailed variation of the holdup and frictional pressure gradients obtained at the vicinity of $1/X^2 \approx 0$ corresponding to low flow rates of the light phase (see the enlargement of this region on Fig. 4c, where the additional two solutions can be observed). The LPF yields triple solutions for co-current down-flow, which are also well predicted by the MTF model. To further substantiate the findings implied by Fig. 4, similar comparisons are shown in Fig. 5 for a steeper inclination of 30°. It is worth noting that the predictions of the experimental holdup by both, the LPF and MTF are better for the case of a steeper inclination. This may imply that fully developed flow conditions in the pipe (as assumed by the models) are more easily approached at steeper inclinations.

A convenient and useful test case is the horizontal laminar flow of equal viscosity fluids, $\tilde{\mu} = 1$. In this case $\widetilde{P}_1 = \widetilde{P}_2$ even with $\rho_1 \neq \rho_2$, and the velocity profile corresponds to single phase, Poiseuille flow at the mixture flow rate $(U_{1s} + U_{2s})$. Simple analytical expressions are then available for the flow rates ratio, dimensionless pressure drop and for the shear stresses (e.g. Ranger and Davis, 1979, Brauner et al., 1996a):

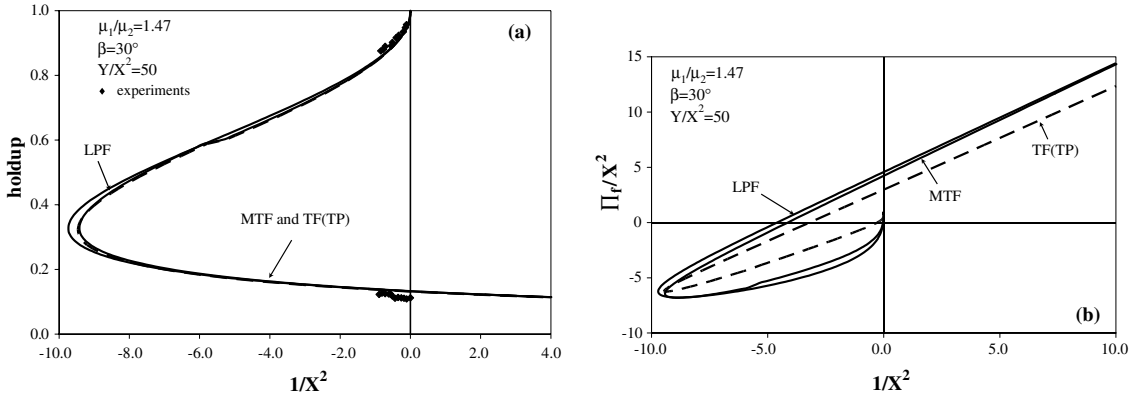

Fig. 5. Comparison of the TF(TP) and the MTF model's predictions with the LPF solution ($\beta = 30°$ and $\tilde{\mu} = 1.47$): (a) Holdup, (b) dimensionless frictional pressure gradient. Experimental data correspond to $Q_1 = 45 \pm 1.5$ ml/min, $\rho_1 = 943.6$ kg/m^3, $\rho_2 = 919.7$ kg/m^3, $\tilde{\mu} = 1.47$ and $\mu_1 = 3.32 \times 10^{-3}$ kg/m/s (Ullmann et al., 2003a).

$$\frac{1}{q}=\frac{U_{2s}}{U_{1s}}=\frac{\pi-\phi_1+\frac{2}{3}\sin 2\phi_1-\frac{1}{12}\sin 4\phi_1}{\phi_1-\frac{2}{3}\sin 2\phi_1+\frac{1}{12}\sin 4\phi_1} \tag{26.1}$$

$$\widetilde{P}_1=\widetilde{P}_2=\widetilde{P}=\frac{U_{1s}+U_{2s}}{U_{2s}}=1+q \tag{26.2}$$

$$\tau_1=\tau_2=\frac{8\mu(U_{1s}+U_{2s})}{D};\quad \tau_i=-\frac{8\mu(U_{1s}+U_{2s})}{D}\cos\phi_1 \tag{26.3}$$

This analytical solution was used also to test the accuracy of the numerical integration scheme employed in the LPF for calculations of the flow rates. As can be seen in Fig. 6, the LPF results for the holdup (and pressure gradient) practically coincide with those obtained by the analytical solution (maximal deviation of 0.04%).

Two fluid models are challenged by this test case, where similar velocities of the two-phases are encountered. The results of MTF model are also shown in Fig. 6a and b. In the scales used in these figures, the results appear identical to those of the analytical expressions given by Eqs. (26). Maximal deviations are less than 1.5% for the pressure gradient and less than 0.5% for the holdup (for the range shown, $X^2 < 10$). These figures demonstrate again the difficulties encountered in applying the TF model for this rather simple case. In the vicinity of $X^2 \approx 1$ a solution can be obtained only if the interface is considered as 'free' with respect to both phases in the calculation of the hydraulic diameters. Very good agreements between the results of the MTF and LPF models for the holdup and pressure gradient are obtained also for horizontal flows with fluids of different viscosities, $\tilde{\mu} \neq 1$ (not shown).

As already demonstrated in Fig. 2, the weaknesses of the TF model become more evident in inclined flows, where a different body force is driving the two layers. In counter current flows, the interaction between the two layers results in back-flow of one of the phases, whereby either the heavier phase is dragged upward, or the lighter phase is dragged downward near the fluids interface. The effects of this backflow on the interfacial shear cannot be adequately represented by the TF model, as is manifested by the discontinuities between the solutions obtained with the different options for representing τ_i and their deviations from the LPF solution. On the other

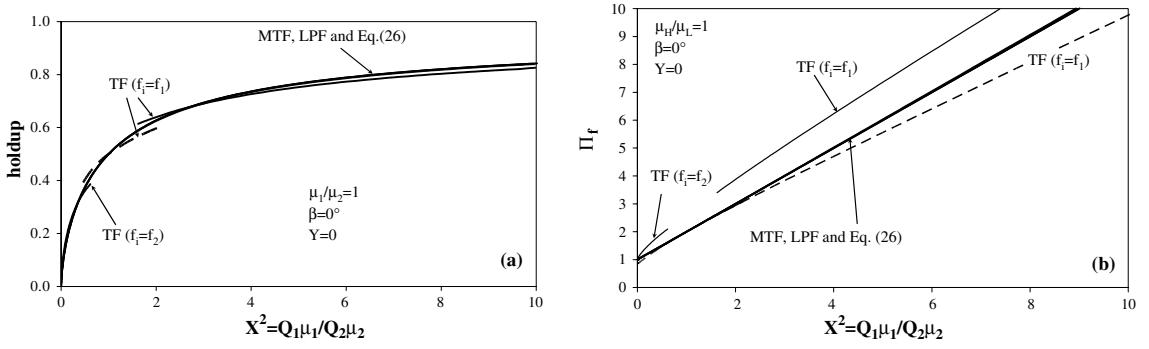

Fig. 6. Validation of the MTF model predictions for the case of horizontal flow with $\tilde{\mu}=1$: Comparison with the exact solution (Eqs. (26.1)–(26.3)) and with the predictions of other stratified flow models: (a) Holdup, (b) dimensionless frictional pressure gradient (dashed line—'free interface' assumed in the hydraulic diameter calculation of both phases).

hand, the closure suggested by the MTF model for τ_i is capable for representing the interaction between the flows in the two layers, and results in continuous predictions of the holdup and pressure drop in the entire solution space, which are also in good agreement with the LPF solution.

In co-current inclined flows backflow can be encountered near the pipe walls. In upward co-current flow, downward back-flow of the heavy phase can be obtained near the lower pipe wall. Similarly, in co-current down-flow, upward backflow of the light phase may result adjacent to the upper wall. Since in the TF model, the wall and interfacial shear stresses are represented in terms of the averaged velocities, the direction of the wall shear stress may be erroneous. These situations can be handled by the MTF model, as the F-interaction factors may attain negative values, and thus affect a change of the direction of the wall shear stress.

This feature of the MTF model is demonstrated in Fig. 7 showing the variation of the F-interaction factors with $1/X^2$ at a constant Y/X^2. This represents variation of the light phase flow rate at a constant flow rate of the heavy phase in a case of co-current up-flow. In this case, the heavy phase is dragged upward by the flow of the light phase. The upper wall shear stress is thus always positive, however, the $F_2 < 1$ implies that its value is lower than that suggested by the TF model. Similarly, the values of $F_i < 1$ suggest a reduced interfacial shear. The most interesting behavior is that of F_1, which changes sign in some range of the light phase flow rate. In the region where F_1 is negative, the wall shear stress exerted on the lower phase is opposite to that expected based on the mean flow direction. The change of sign is associated with the backflow of the heavier phase. Indeed, when the shear exerted by the lighter phase is not sufficiently high, backflow of the heavier phase is encountered, resulting in a reversed, upward directed wall shear stress. The velocity profile obtained by the LPF solution in this region (Fig. 7b) shows the backflow.

The correction introduced by the F_1-interaction factor become more significant as the inclination parameter is increased and gravity effects become more dominant. Fig. 8 reveals that at relatively high flow rates of the light phase, three different values for F_1 correspond to a specified flow rates ratio: one positive value and two negative values. These three values are associated with

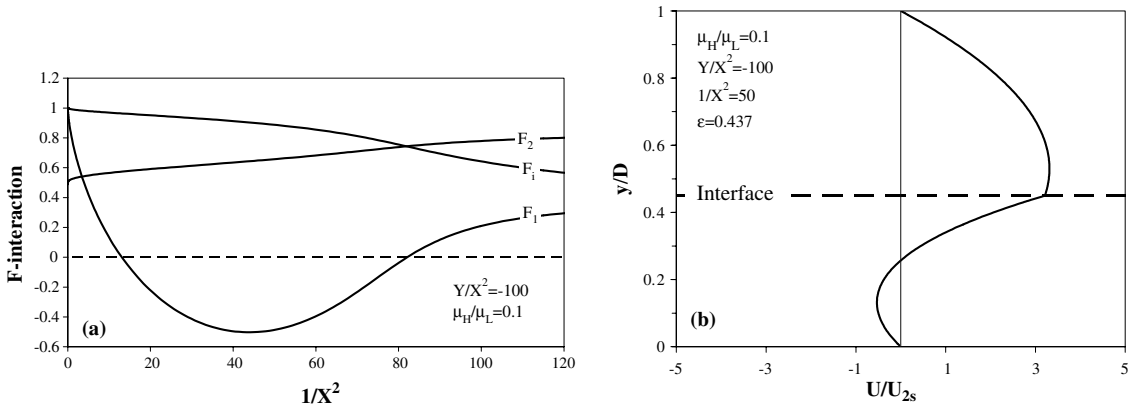

Fig. 7. (a) Variation of the MTF F-interaction factors with the light phase flow rate in the case of co-current up-flow, $Y/X^2 = -100$, $\tilde{\mu} = 0.10$. (b) The LPF solution for the velocity profile at the pipe center line for $1/X^2 = 50$.

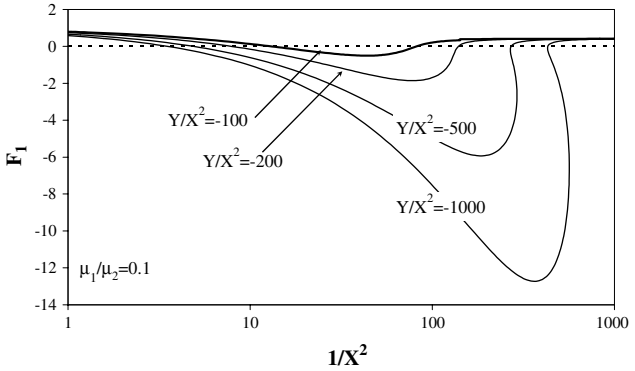

Fig. 8. Effect of the inclination parameter on the MTF F_1-interaction factor in the case of co-current up-flow, $\tilde{\mu} = 0.10$.

the triple solution for the holdup in this range of flow rates ratios. The holdup curve for a test case of constant, low flow rate of the heavy phase, corresponding to $Y/X^2 = -1000$, is shown in Fig. 9. This figure shows also the velocity profiles corresponding to the three solutions (A, B, C) at $1/X^2 = 600$ (obtained by the LPF solution). Inspection of the velocity profiles reveals that only

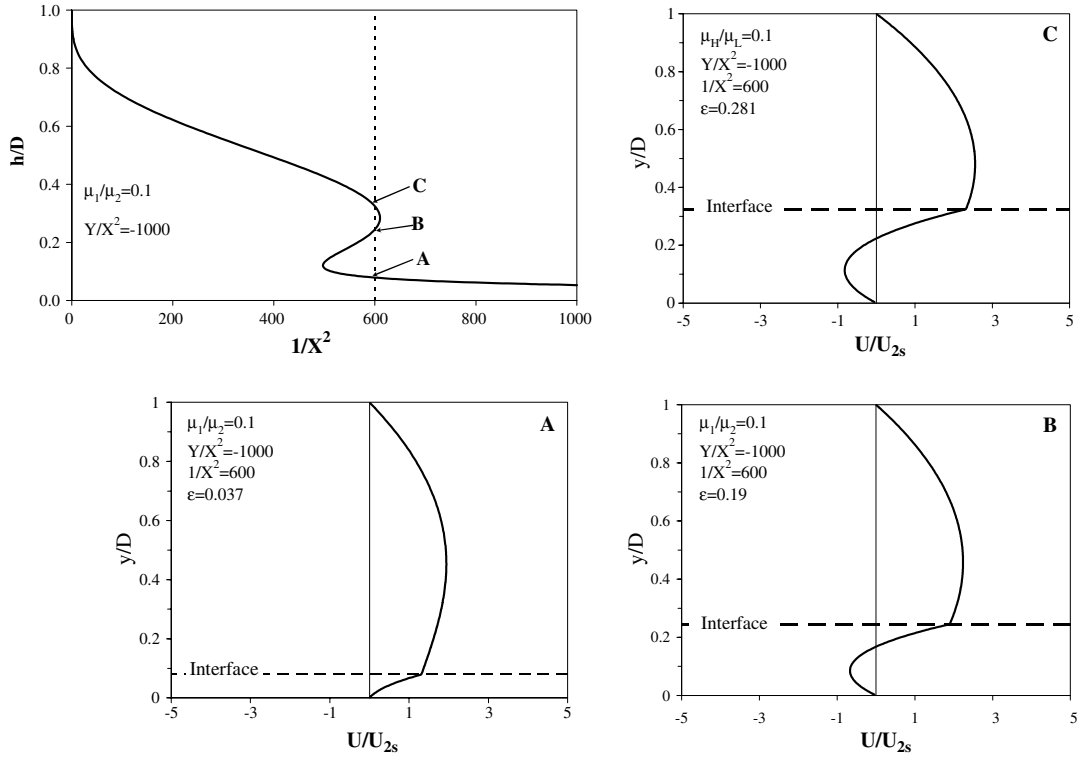

Fig. 9. The LPF velocity profiles at the pipe center line for the triple holdups obtained with co-current up-flow—$Y/X^2 = -1000$, $\tilde{\mu} = 0.10$, at $1/X^2 = 600$ ($u/U_{2s} < 0$ indicates backflow).

with the lowest holdup (A), the shear exerted by the light phase is sufficient to drag upward the entire flow of the heavy phase (no backflow). For the two higher holdups (B and C), backflow of the heavy phase results at the lower wall. Therefore, with these two holdups, the lower wall shear stress is reversed, in accordance with the negative values of the F_1 interaction factor indicated by the MTF model for these holdups.

In fact, multiple holdups are obtained with all the above stratified flow models (LPF, TP, TF and MTF) in some range of operational variables. Multiple (double) holdups are inherent in counter-current flows (Ullmann et al., 2003a), up to the flooding point, beyond which no solution is obtained. In co-current upward or downward flows, however, multiple (triple) holdups correspond to a limited range of operational conditions. The possibility of obtaining multiple holdups in co-current up-flow was recently verified experimentally (Ullmann et al., 2003b). Fig. 10 shows the LPF model results for the variation of the holdup curves with the inclination parameter. The counter-current region diminishes with the decrease of the inclination parameter. The triple solution for downward flow ($Y/X^2 > 0$) is typically obtained for small positive value of $1/X^2$ corresponding to high flow rates of the heavy phase and/or low flow rates of the light phase (see the detailed picture shown in Fig. 10). The triple solutions for upward flows ($Y/X^2 < 0$) are in the range of relatively high $1/X^2$ (see for example Fig. 9). These characteristics are similar to those predicted by the TP model and discussed in Ullmann et al., 2003b. It is worth noting that in case of multiple solutions, computational software usually yields only one of the solutions for specified operational conditions. Therefore, a prior mapping of the multiple solution regions can help in identifying the operational conditions for which multiple solutions should be expected. In these regions the user should check whether the solution obtained by the computational code is the relevant one for the particular application, and to examine the physical significance of the other possible solutions.

The procedure for mapping the multiple holdup boundaries of the LPF solution are demonstrated in Fig. 11. For a specified value of inclination parameter and $\tilde{\mu}$, the range of X^2 corresponding to multiple holdups is bounded by the values of X^2 where $\mathrm{d}X^2/\mathrm{d}\varepsilon = 0$. The

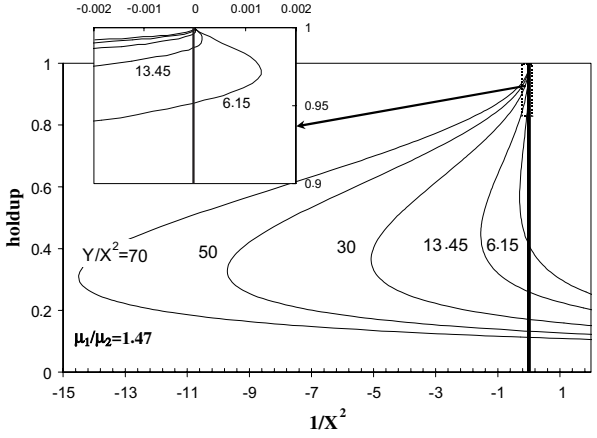

Fig. 10. The effect of the inclination parameter on the holdup curves obtained by the LPF solution.

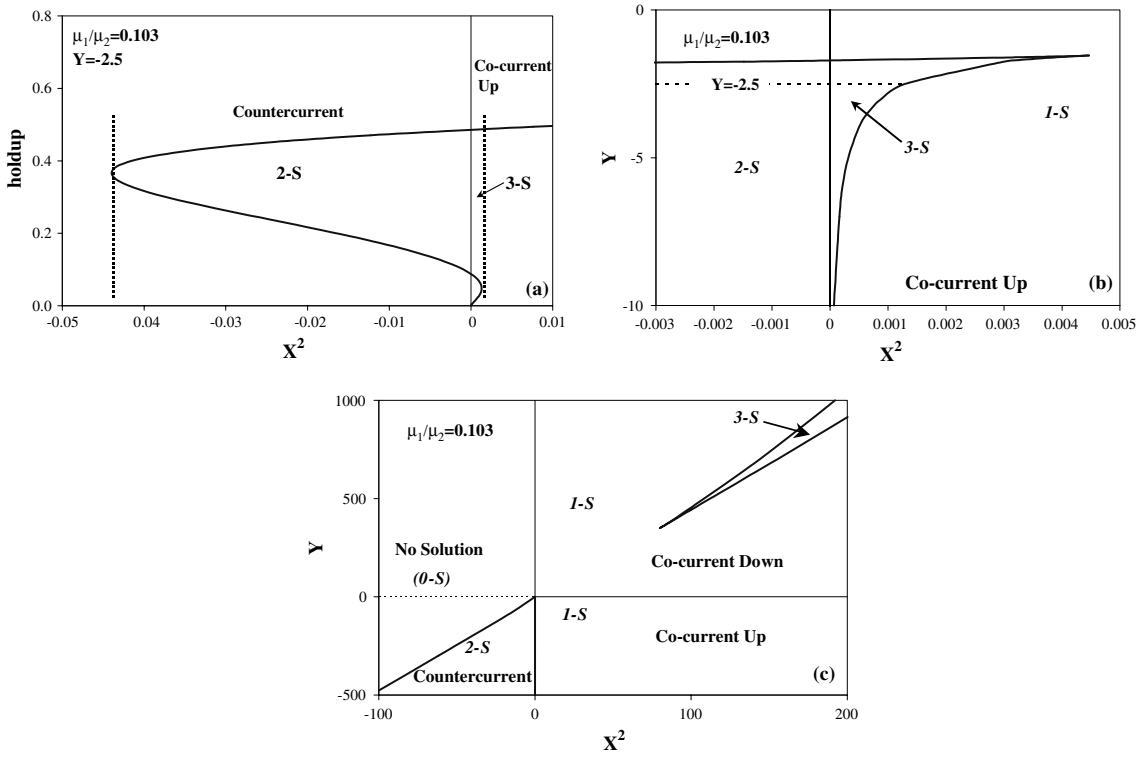

Fig. 11. Boundaries of the multi-valued holdups in the LPF solution for counter-current and co-current flow with $\tilde{\mu} = 0.103$.

counter-current flow range ($X^2 < 0$) is associated with a double solution for the holdup ($2 - S$). As shown in Fig. 11c, for any given negative X^2, there is a maximum value of Y for which counter-current flow is feasible. Co-current flow is feasible in the whole range of positive X^2 (at least $1 - S$). The triple solution range ($3 - S$) of co-current downward flow is clearly seen in the figure. The range of triple solution for upward co-current flow is for small positive values of X^2 (adjacent to $X^2 = 0$, as detailed in Fig. 11b).

The effects of the viscosity ratio on the multiple-holdup regions obtained by the LPF solution are summarized in Fig. 12. Fig. 12b is for upward flows, showing the multiple-holdup boundaries in terms of Y/X^2 vs. $1/X^2$. The upper part of this figure (Fig. 12a) is actually a mirror image of its lower part and represents the ranges where triple solution exists in co-current downward flows in terms of Y vs. X^2. Fig. 12a and b demonstrate the complete similarity between the LPF stratified flow solutions in upward and downward co-current flows. It clearly indicates that there is a minimal X^2 (or minimal $1/X^2$) for co-current downward (or co-current upward) flows for which triple solutions can be obtained. It is important to emphasize that Fig. 12 provides a mapping of the dimensionless parameters for which triple solutions are obtained in laminar co-current stratified up and down flows with a flat and smooth interface. The relevance of the triple solution region for a particular application (specified densities, viscosities, tube diameter and inclination) can be examined after transforming the Y/X^2 vs. $1/X^2$ boundaries to the corresponding U_{1s} vs. U_{2s}

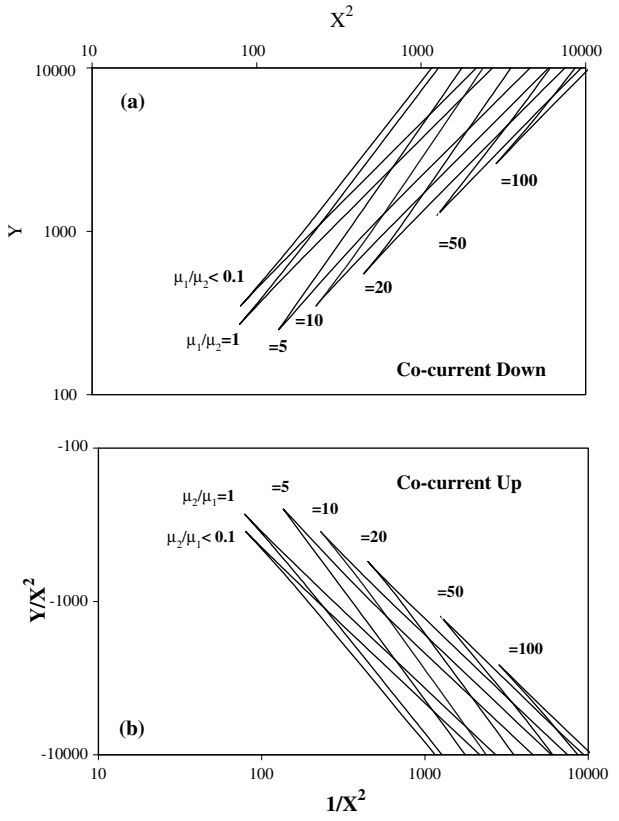

Fig. 12. The effect of the viscosity ratio on the boundaries of the triple holdups regions in the LPF solution: (a) co-current down-flow, (b) co-current up-flow.

boundaries. The stability of the solutions can be then examined by stability analysis techniques or in view of an experimental flow pattern map. It should be mentioned that the stability of the stratified flow is dependent on additional dimensionless parameters. However, the introduction of the triple-solution region on the flow pattern maps of gas–liquid and liquid–liquid systems indicates that these regions are relevant, and may be related to transition to stratified flow. In particular, in co-current gas–liquid up-flow, the restricted small range of flow rates where stratified flow exists may be associated with the triple solution region (Ullmann et al., 2003b).

Comparisons of the multiple solution region predicted by the various stratified flow models in the case of co-current up-flow are demonstrated in Fig. 13 for viscosity ratios of 0.1 and 10. The triple solution boundaries of the LPF and MTF models are shown to be very similar. Therefore, it can be concluded that the MTF model can substitute the complicate LPF model also for the mapping of the multiple solution regions. However, using the MTF model for this purpose still requires a tedious procedure. The easiest way to obtain the multiple solutions boundaries is by the TP model, which provides analytical expressions for the multiple holdup boundaries (Ullmann et al., 2003b). As shown in Fig. 13, the TP multiple solution regions can provide reasonable estimates for the operational zones were multiple holdups are to be expected in pipe flow.

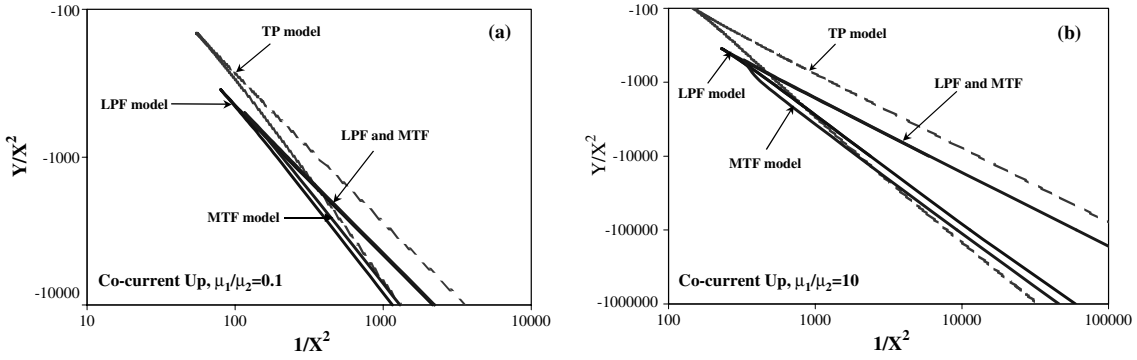

Fig. 13. Comparison of the triple solution boundaries in the LPF, MTF, and TP models: (a) $\tilde{\mu} = 0.10$, (b) $\tilde{\mu} = 10$.

5. Conclusions

The exact solution for fully developed laminar pipe flow (LPF) in inclined tube is used to study the effect of inclination on the characteristics of counter-current and co-current stratified flows. This solution is used also to examine the validity of results for the holdup and pressure drop obtained by two-fluid (TF) models. It is shown that the common practice of using single-phase-flow-based closure relations for the shear stresses in TF models is problematic in horizontal flows, and fails in predicting the holdup and pressure drop in co-current and counter-current inclined flows. The expressions obtained for the wall and interfacial shear stresses in the LPF exact solution are however too complicated to suggest practical closure relations for two-fluid models.

The simple two-plate (TP) model was used to derive new closure relations, which account for the interaction between the phases. The new closure relations are formulated in terms of the single-phase-based expressions, which are augmented by the two-phase interaction factors.

The so-obtained modified two-fluid (MTF) model was tested against the LPF exact solution. Very good results were obtained for the pressure drop and holdup for a wide range of dimensionless parameters in co-current and counter-current laminar flows. The MTF model is also capable of handling the change in the direction of the wall shear-stress when gravity driven backflow of either of the phases is encountered. The MTF closure relations can be applied for the calculations of undeveloped conditions and slow transients in stratified laminar pipe flows. In such cases, the MTF closure relations should be expressed in terms of local/instantaneous values of the holdup and phases velocities. Although these closure relations are valid for a smooth and flat interface, they can provide a useful platform for introducing necessary corrections in cases these assumptions are not strictly met.

The boundaries of multiple (triple) holdup regions in co-current upward and downward inclined flows are mapped in terms of the flow dimensionless parameters, i.e. the inclination parameter vs. the Martinelli parameter for a specified viscosity ratio. The regions obtained via the LPF exact solution and the MTF model practically coincide.

Further research is currently conducted to extend the MTF model to turbulent flows in one or both layers.

Appendix A

The Fourier integrals in Eqs. (10.1) and (10.2) are given by

$$I_1^1 = \int_0^\infty W_1 \cos(\omega\xi)\,\mathrm{d}\omega; \quad W_1 = \frac{\sinh[\omega(\phi_1+\phi)]}{\sin(\omega\pi)\cosh(\omega\phi_1)} \tag{A.1}$$

$$I_2^1 = \int_0^\infty W_2 \cos(\omega\xi)\,\mathrm{d}\omega; \quad W_2 = \frac{\sinh[\omega(\phi_2-\phi)]}{\sinh(\pi\omega)\cosh(\omega\phi_2)} \tag{A.2}$$

$$I_1^2 = \int_0^\infty \frac{\psi_1}{\psi} W_1 \cos(\omega\xi)\,\mathrm{d}\omega; \quad \psi_1 = \sin\phi_1 - \frac{tg(\omega\phi_1)}{\omega}\cos\phi_1 \tag{A.3}$$

$$I_2^2 = \int_0^\infty \frac{\psi_2}{\psi} W_2 \cos(\omega\xi)\,\mathrm{d}\omega; \quad \psi_2 = \sin\phi_2 - \frac{tg(\omega\phi_2)}{\omega}\cos\phi_2 \tag{A.4}$$

$$I_1^3 = \int_0^\infty \frac{\psi_2}{\psi} W_1 \cos(\omega\xi)\,\mathrm{d}\omega \tag{A.5}$$

$$I_2^3 = \int_0^\infty \frac{\psi_1}{\psi} W_2 \cos(\omega\xi)\,\mathrm{d}\omega \tag{A.6}$$

where:

$$\psi(\omega) = \frac{tgh(\omega\phi_1)}{\omega} + \tilde{\mu}\frac{tgh(\omega\phi_2)}{\omega} \tag{A.7}$$

The results obtained after integration over the phases flow cross-sectional area, using the Jacobian $J(\xi,\phi)$ defined in Eq. (6.3), are

$$I_1^{Aj} = \int_{-\phi_1}^0 \int_{-\infty}^\infty I_1^j J(\xi,\phi)\,\mathrm{d}\xi\,\mathrm{d}\phi; \quad j = 1,2,3 \tag{A.8}$$

$$I_2^{Aj} = \int_0^{\phi_2} \int_{-\infty}^\infty I_2^j J(\xi,\phi)\,\mathrm{d}\xi\,\mathrm{d}\phi; \quad j = 1,2,3 \tag{A.9}$$

$$I_1^{A4} = \frac{1}{2}\int_{-\phi_1}^0 \int_{-\infty}^\infty \frac{\sin(\phi_1+\phi)}{\cosh\xi+\cos\phi} J(\xi,\phi)\,\mathrm{d}\xi\,\mathrm{d}\phi \tag{A.10}$$

$$I_2^{A4} = \frac{1}{2}\int_0^{\phi_2} \int_{-\infty}^\infty \frac{\sin(\phi_2-\phi)}{\cosh\xi+\cos\phi} J(\xi,\phi)\,\mathrm{d}\xi\,\mathrm{d}\phi \tag{A.11}$$

Note that integration in (A.10) and (A.11) can be carried out analytically (Ranger and Davis, 1979).

$$I_1^{A5} = I_1^{A2} + \cos\phi_1 I_1^{A1} - I_1^{A4} \tag{A.12}$$

$$I_2^{A5} = \tilde{\mu} I_2^{A2} + \cos\phi_2 I_2^{A1} - I_2^{A4} \tag{A.13}$$

$$I^{A6} = I_1^{A5} - \tilde{\mu} I_1^{A3} \tag{A.14}$$

$$I^{A7} = I_1^{A5} I_2^{A5} - \tilde{\mu} I_1^{A3} I_2^{A3} \tag{A.15}$$

References

Bentwich, M., 1964. Two-phase axial flow in pipe. Trans. ASME Ser. D 86, 669–672.

Biberg, D., Halvorsen, G., 2000. Wall and interfacial shear stress in pressure driven two-phase laminar stratified pipe flow. Int. J. Multiphase Flow 26, 1645–1673.

Brauner, N., Moalem Maron, D., 1989. Two-phase liquid–liquid stratified flow. Physico-Chem. Hydrodyn. 11, 487–506.

Brauner, N., Rovinsky, J., Moalem Maron, D., 1995. Analytical solution of laminar–laminar stratified two-phase flows with curved interfaces. Proc. 7th Int. Meeting Nucl. Reactor Thermal-Hydraul. NURETH 7, 192–211.

Brauner, N., Rovinsky, J., Moalem Maron, D., 1996a. Analytical solution for laminar–laminar two-phase flow in circular conduits. Chem. Eng. Commun. 141–142, 103–143, A. Dukler memorial issue.

Brauner, N., Rovinsky, J., Moalem Maron, D., 1996b. Determination of the interface curvature in stratified two-phase systems by energy considerations. Int. J. Multiphase Flow. 22, 1167–1185.

Brauner, N., Rovinsky, J., Moalem Maron, D., 1998. A two-fluid model for stratified flows with curved interfaces. Int. J. Multiphase Flow 24, 975–1004.

Goldstein, A., 2002. Analytical solution of two-phase laminar stratified flow in inclined tubes. M.Sc. Thesis, Tel-Aviv University, Israel.

Gorelik, D., Brauner, N., 1999. The interface configuration in two-phase stratified flow. Int. J. Multiphase Flow 25, 877–1007.

Landman, M.J., 1991. Non-unique holdup and pressure drop in two-phase stratified inclined pipe flow. Int. J. Multiphase Flow 17, 377–394.

Moalem-Maron, D., Brauner, N., Rovinsky, J., 1995. Analytical prediction of the interface curvature and its effects on the stratified two-phase characteristics. In: Proceedings of the International Symposium Two-Phase Flow Modeling and Experimentation, vol. 1. pp. 163–170.

Ranger, K.B., Davis, A.M.J., 1979. Steady pressure driven two-phase stratified laminar flow through a pipe. Can. J. Chem. Eng. 57, 688–691.

Semenov, N.L., Tochigin, A.A., 1962. An analytical study of the separate laminar flow of a two-phase mixture in inclined pipes. J. Eng. Phys. 4, 29.

Ullmann, A., Zamir, M., Ludmer Z., Brauner, N., 2001. Flow patterns and flooding mechanisms in liquid–liquid countercurrent flow in inclined tubes. In: Proceedings of the third ICMF, New Orleans.

Ullmann, A., Zamir, M., Ludmer, Z., Brauner, N., 2003a. Stratified laminar counter current flow of two liquid phases in inclined tube. Int. J. Multiphase Flow 29, 1583–1604.

Ullmann, A., Zamir, M., Gat, S., Brauner, N., 2003b. Multi-holdups in co-current stratified flow in inclined tubes. Int. J. Multiphase Flow 29, 1565–1581.